Automated Damage and Defect Detection with Low-Cost X-Ray Radiography using Data-driven Predictor Models and Data Augmentation by X-Ray Simulation

Stefan Bosse [1,2]

[1] University of Bremen, Dept. Mathematics & Computer Science, Bremen, Germany
[2] University of Siegen, Dept. of Mechanical Engineering, Siegen, Germany

sbosse@uni-bremen.de

Introduction

Detection of hidden defects and damages in materials using X-ray images is still a challenge. Often a lot of defects are not directly visible by visual inspection.

Introduction

Detection of hidden defects and damages in materials using X-ray images is still a challenge. Often a lot of defects are not directly visible by visual inspection.

In this work, a data-driven feature marking model is introduced performing semantic pixel annotation in X-ray images.

Features are:

Pores, Delaminations, Cracks, or general anomalies

Introduction

- For example, an impact damage in laminate structures can be nearly invisible by a frontal X-ray projection, although, the deformation can be seen and detected manually by hand perception.
- Hidden pores in die casted materials can be detected and analyzed by 3D CT volume rendering, but hard to be identified in single projection images (Radiography).
- Things are getting more worse if a portable low-cost X-ray radiography or semi-tomography machine is used (called Low-Q measuring device), as introduced and described in this work.

> It is desirable to detect or mark defects, damages, or impurities by an automated feature marking system directly in the measured images. The impact of image quality can be relevant to the feature detection quality, regardless of the complexity of the model behind

Introduction

Goals of this work

1. Detect hidden defects in homogeneous metal materials by using single projection X-ray radiography images
2. Transition from industrial non-portable, heavy, and expensive X-ray measuring devices (>500k€) towards mobile, lightweight, portable, and low-cost X-ray radiography systems (< 1k€)

X-ray Measuring Devices

Basically we can classify X-ray measuring devices and systems into three classes with respect to Non-destructive Testing (NDT) in engineering, especially for metals and composite materials:

1. **High-Q** Micro-CT devices with micro focus tubes and optional optical magnification
   Focal spot diameter below 50 µm
   direct imaging SSD detector with resolution above 100µm, but effective resolution below 100µm, SNR > 200;

2. **Mid-Q** Industrial systems
   Focal spot diameter above 200 µm, typically 0.8 mm
   Direct imagining SSD detectors, detector resolution above 100µm, effective resolution above 100µmSNR > 100;

3. **Low-Q** Low-cost system (standard focal spot diameter above 800 µm, typically 0.8 mm), effective resolution typically above 50µm, SNR < 50.

X-ray Measuring Devices

An X-ray measuring system consists of:

1. X-ray source (commonly cone beam with a specific focal size diameter *fsd*) , a X-ray tube with
    - cold-emission
    - hot-emission (Coolidge)

> In cold-emission, the electrical field extracts and accelerates electrons from the cathode to the anode, in hot-emission there is a heated free electron source, and the electrical field only accelerates the electron to a target anode material. Cold emission tubes lack independent tube current control (dependent on the tube voltage).

X-ray Measuring Devices

2. X-ray detector.
    - direct conversion system
    - indirect conversion system, directly coupled
    - indirect and imaging system, indirectly coupled

> In a direct conversion system the X-ray photons will generate electrons (photo effect) directly in the solid-state device, in an indirect conversion system a conversion material (scintillator) is required to convert X-ray photons into visible light photons, finally converted to electrons in a solid-state detector.

Solid-state detectors are typically Coupled Charge Devices (CCD) or CMOS pixel detectors. Although, used in an indirect conversion system sensitive to visible light, the are still sensitive to incident X-ray radiation producing shot or popcorn noise.

Low-Cost X-Ray Device

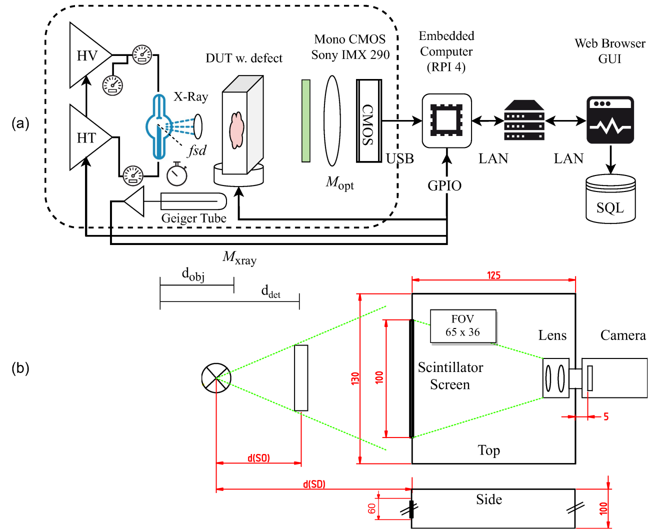

Fig. 1. Low-cost X-ray Radiography and CT instrument (a) General overview (b) Details of the detector (all dimensions in mm)

Low-Cost X-Ray Device

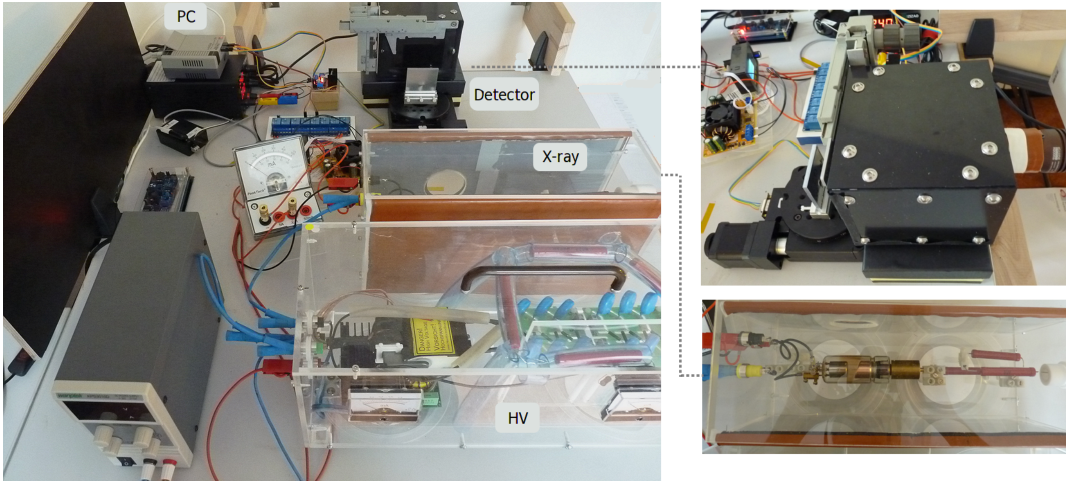

Fig. 2. Prototype of the low-cost X-ray Radiography and CT instrument

Low-Cost X-Ray Device

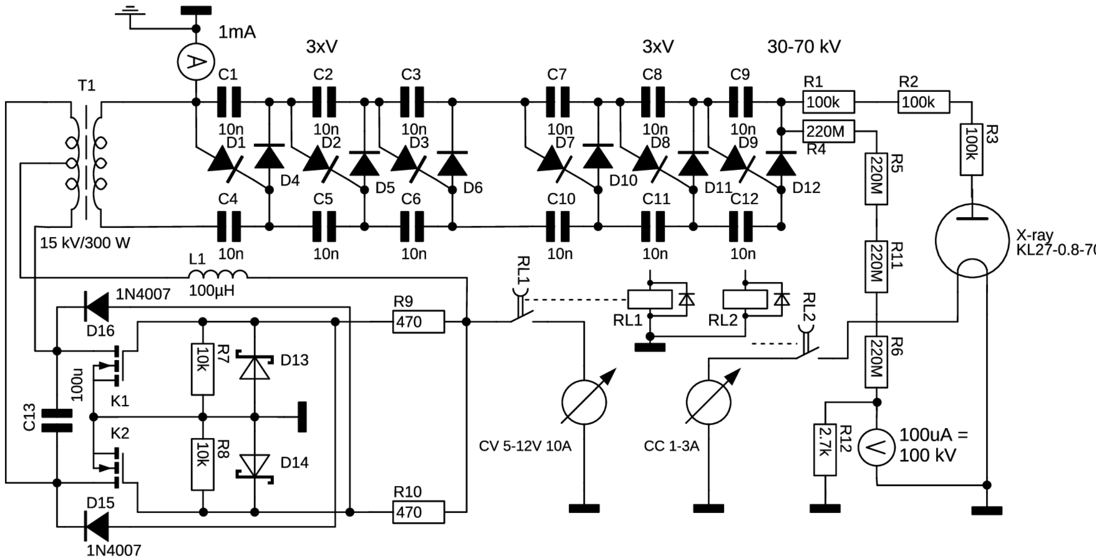

Fig. 3. Electronic schematic of the low-cost X-ray source

Detector

The resolution of an X-ray detector system is limited mainly by two parameters:

1. Detector pixel size d_{p} multiplied by the optical image magnification, i.e., $d_{\mathrm{p}} M_{\mathrm{opt}}$;
2. The X-ray magnification M_{xray};
3. The geometrical unsharpness a with increasing M_{xray} wrt. to the focal spot diameter f_{b}.

The X-ray magnification and unsharpness (resolution limit) is given by:

$$M_{xray} = \frac{d_{src,\mathrm{det}}}{d_{src,obj}}$$

$$a = \left(\frac{d_{obj,\mathrm{det}}}{d_{\mathrm{det},src}} \right) f_b$$

Scintillator

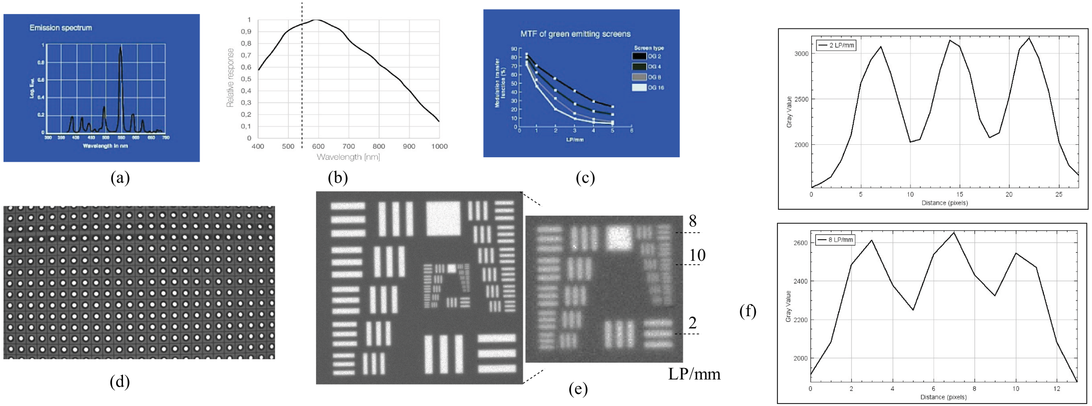

Fig. 4. (a) Emission spectrum of the scintillator material [CAW23] (b) Spectral sensitivity of the IMX290 image sensor [FRA19] (c) Resolution of the scintillator screen in dependence of the material thickness and amplification factor [CAW23] (OG-2: conversion factor 100, OG-4: 200, and so on) (d) Dot pattern measured with Low-Q X-ray detector (e) USAF 1951 pattern recorded with 55 kV/0.7 mA/average of 4 images (f) Intensity profiles and contrast at 2 an 8 LP/mm from (e)

Noise

- The exposure time t_x defines the noise level and the signal-to-noise ratio (SNR) achievable with the given X-ray power P_x.

- The industrial reference Mid-Q system has a pixel area size of about 40 kμm ^{2}, whereas the Low-Q detector has a pixel area of only 9μm ^{2}!

- The direct imaging Mid-Q system has a tight coupling of the scintillator to the detector pixels via a FOP (low attenuation), whereas the indirect imaging system poses optical losses in lenses and coupling components.

- The Mid-Q system requires typically exposure times in the order of 100 ms (with P_x=200 W), whereas the Low-Q device requires at least 5000 ms (with P_x=50 W).

More Noise

- The CMOS image sensor is sensitive to X-ray radiation, not too much to use the image sensor directly, but with respect to popcorn and shot noise.

    - Popcorn noise is a random seed phenomenon, i.e., in some pixels there is an electron wall breakthrough leading to saturated (white) pixels. Fortunately, after the pixels are cleared (before the sampling of the next image), the saturation is eliminated and two succeeding images will commonly not pose the same flooded pixels.

- Commonly, the image device is not directly exposed the X-ray beam. Instead, a mirror under an angle of 45° is used and the camera is placed with a 90° angle with respect to the X-ray beam axis (see [BAL22], for example). We tried the same approach, but we observed:

1. An expected reduction of light intensity (mirror reflectivity < 1) and more geometric distortions;
2. There is still shot noise (although, strongly reduced, but not totally vanished).

More Noise

Therefore, we placed the camera again in the X-ray beam and using a simple multi-image noise compensation method. It removes shot noise, and reduces non-gaussian X-ray and gaussian (electronics) noise, too.

More Noise

Therefore, we placed the camera again in the X-ray beam and using a simple multi-image noise compensation method. It removes shot noise, and reduces non-gaussian X-ray and gaussian (electronics) noise, too.

Choosing the γ threshold is crucial because not all shot noise pixels reach the maximum camera intensity, and some will only be reduced by averaging if they are below the chosen threshold.

More Noise: Reduction Algorithm

```
σ0 := Σ[1]
∀ (x,y) ∈ coord(σ0) do
  if σ0[x,y] > γ then
    ∀ σ ∈ { Σ / σ0 } do
      if σ[x,y] < γ then
        σ0[x,y] := σ[x,y]
        break
      endif
    done
  endif
  ∀ σ ∈ { Σ / σ0 } do
    if σ[x,y] < γ then
      σ0[x,y] := σ0[x,y] + σ[x,y]
    else
      σ0[x,y] := σ0[x,y] + σ0[x,y]
    endif
  done
  σ0[x,y] := σ0[x,y] / |Σ|
done
```

Alg. 1. Shot (popcorn) noise removal and image averaging. γ is a noise threshold with respect to the image pixel value range (commonly 0.9*max*) and Σ is a set of images. The result of the averaged and noise corrected image is σ_0

More Noise: Reduction Algorithm

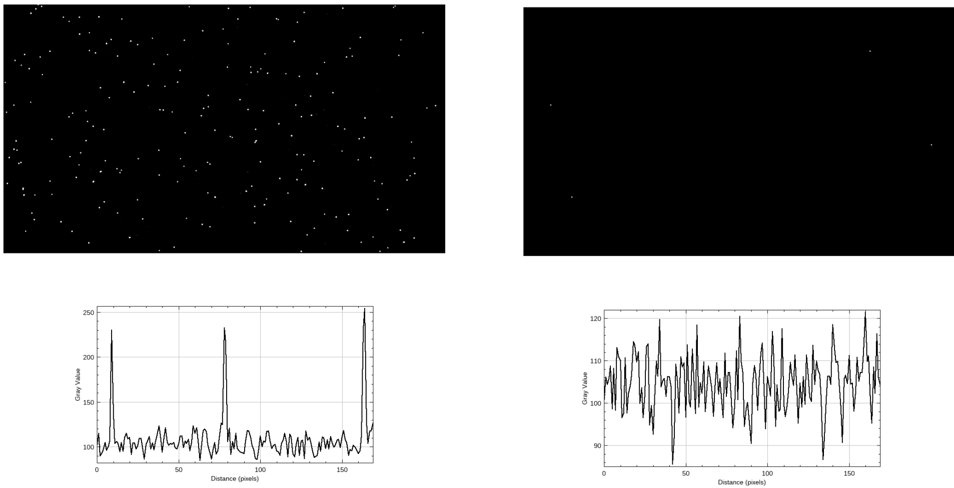

(a) Without Noise Cancellation

(b) With Noise Cancellation (2 Im.)

Fig. 5. (Top) Example images without (left) and with (right) noise cancellation (Bottom) Example line intensity plots with flooded pixels (left) and residual noise only (right)

X-ray Image Simulation

As common in engineering applications, the data variance of experiments and specimens is limited.

X-ray Image Simulation

As common in engineering applications, the data variance of experiments and specimens is limited.

- Specimens with impacts damages pose a wide range of different micro and macro damages, e.g., delaminations, cracks, kissing bond defects, and many more. Therefore, the measurement (X-ray image) of one specimen delivers only a few features, and the number of specimens is limited, too.
- High-pressure Die casted aluminum specimens contain a high number of gas pores (here named defects), and the number of specimens can be high.

X-ray Image Simulation

As common in engineering applications, the data variance of experiments and specimens is limited.

- Specimens with impacts damages pose a wide range of different micro and macro damages, e.g., delaminations, cracks, kissing bond defects, and many more. Therefore, the measurement (X-ray image) of one specimen delivers only a few features, and the number of specimens is limited, too.

- High-pressure Die casted aluminum specimens contain a high number of gas pores (here named defects), and the number of specimens can be high.

Even if the feature and data variance is sufficient, there is no ground truth of the data, especially required for accurate labelling of training data for supervised Machine Learning (ML).

X-ray Image Simulation

> For this reason, in this work X-ray images are computed (simulated) numerically from synthetic specimens based on a CAD model and Monte-Carlo simulation techniques.

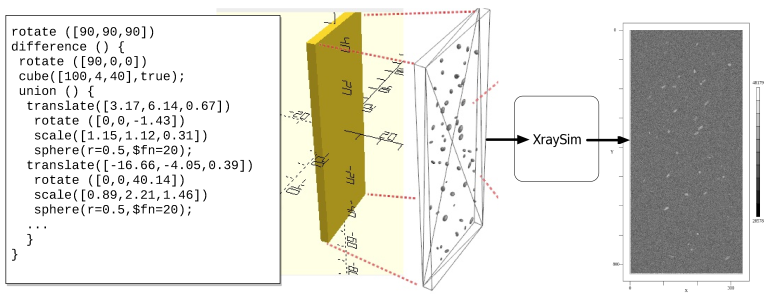

Fig. 6. Modelling of a die casted aluminum plate with gas pores using Monte Carlo simulation. Geometric parameters of real measure pores are used to create synthetic pores at random positions. (Left) Programmatic CSG model (Center) Rendered 3D model with synthetic pores / holes (Right) Simulated X-ray Image

Feature Detector: Semantic Pixel Classifier

The main objective of this work is to use an automated feature detector applied to single projection X-ray images delivered by a Low-Q (low-cost) X-ray instrument to detect hidden defects in materials, here specifically pores in high-pressure die casted aluminum plates.

Feature Detector: Semantic Pixel Classifier

The main objective of this work is to use an automated feature detector applied to single projection X-ray images delivered by a Low-Q (low-cost) X-ray instrument to detect hidden defects in materials, here specifically pores in high-pressure die casted aluminum plates.

- The input is an X-ray image, the output is a feature map image that marks pores (binary classifier) and provides the geometric parameters and position
- A pixel classifier is commonly implemented with a Convolutional Neural Network (CNN), mostly with only one or two convolution-pooling layer pairs.
  - The input of the CNN is a sub-window masked out from the input image at a specific center position (x,y). The output is a class (or a real value in the range [0,1] as an indicator level for a class). The neighbouring pixels determine the classification result. th window with the CNN application is moved over the entire input image producing the respective feature output image.

Feature Detector: Semantic Pixel Classifier

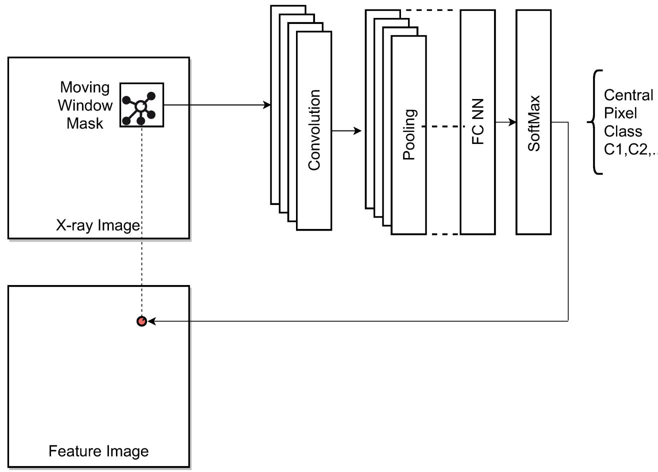

Fig. 7. Semantic pixel classifier applied to X-ray single projection images to detect and mark hidden defects

Results

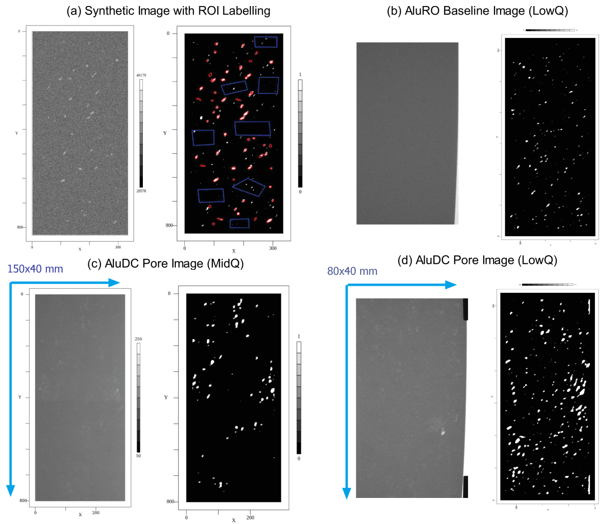

Fig. 8. Feature marking for different X-ray images using two measuring instruments and synthetic images. Low-Q images have a different scaling and region compared to the Mid-Q and synthetic X-ray images. aluDC: Die casted aluminum plate with pores, aluRO: Rolled and polished aluminum plate without pores.

Results

> ⚠ The pixel classifier was trained with synthetic images and applied to real images.

1. The semantic pixel classifier marks about 95% of the pores in the synthetic X-ray image

2. The density (probability?) of marked pores in the Low-Q images are higher compared with images from Mid-Q device

3. But! The semantic pixel classifier is sensitive to X-ray noise ⇒ The AluRO probe shows false predictions (expected: no predictions because there are no pores)

Conclusions

But overall the pixel classifier trained with synthetic simulated X-ray images is able to detect pores in X-ray single projection images even in the case of the Low-Q device!

Conclusions

✔ But overall the pixel classifier trained with synthetic simulated X-ray images is able to detect pores in X-ray single projection images even in the case of the Low-Q device!

✖ The semantic pixel detector is sensitive to noise (although, significant Gaussian noise was added to the training examples)

Conclusions

- ✔ But overall the pixel classifier trained with synthetic simulated X-ray images is able to detect pores in X-ray single projection images even in the case of the Low-Q device!

- ✖ The semantic pixel detector is sensitive to noise (although, significant Gaussian noise was added to the training examples)

- ✔ The Low-Q measuring device competes with a 500 times more expensive industrial measuring device.

End.

Thank you for your attention. All questions are welcome!

Automated Damage and Defect Detection with Low-Cost X-Ray Radiography using Data-driven Predictor Models and Data Augmentation by X-Ray Simulation

Further information can be found here: http://edu-9.de